Supporting Information

Ellingsgaard *et al.* 10.1073/pnas.0801059105

SI Materials and Methods

Animals. Male C57BL/6J mice (Harlan) were used for all mouse islet experiments. Wistar Kyoto rats were purchased from Janvier. For high-fat diet studies, C57BL/6J wild-type and B6;129S2-*Il6*^{tm1Kopf}/J (IL-6 KO) mice backcrossed for 11 generations and maintained on a C57BL/6J background were obtained from the Jackson Laboratory. Animals were fed a hypercaloric (high-fat [HF]) diet manufactured by Research Diets. The HF diet contained 58%, 26%, and 16% calories from fat, carbohydrate, and protein, respectively, and a total of 5.6 kcal/g. The control diet was manufactured by Provimi Kliba AG and contained 29%, 39%, and 32% calories from fat, carbohydrate, and protein, respectively, and a total of 2.8 kcal/g. Guidelines for the use and care of laboratory animals at the University of Zurich were followed, and ethical approval was granted by the Zurich Cantonal Animal Experimentation Committee.

Islet Isolation and Culture. Human islets were isolated from pancreata of organ donors at the University of Geneva Medical Center, Switzerland, and at INSERM ERIT-M 0106, Lille, France. Mouse and rat islets were isolated from C57BL/6J mice and Wistar rats, respectively, by collagenase digestion (Worthington), using modifications of procedures described previously (1). Human and mouse islets were cultured as previously reported on extracellular matrix–coated plates (Novamed) in CMRL 1066 and RPMI 1640 media respectively, 10% FCS and antibiotics (2). For proliferation studies, islets were cultured in the presence of BrdU (final concentration 10 μM) and IL-6 (1–200 ng/ml). For some proliferation experiments, islets were dispersed into single cells at the end of the treatment using Trypsin (Invitrogen), followed by BrdU and glucagon/insulin co-staining. The IL-6 receptor antagonist, super antagonist 7 (Sant7), was kindly provided by Sigma Tau (3). For apoptosis studies, islets were dispersed into single cells before treatment with 0.5 mM palmitate (Sigma) and 33.3 mM glucose. In some conditions, cells were pretreated with 100 ng/ml IL-6 for 1 h before and during treatment.

α- and β-Cell Isolation and Culture. Islet α- and β-cells (purity $\approx$90% as assessed by insulin and glucagon staining, respectively) were purified from male Wistar rats (150–250 g, 6–11 weeks of age) as previously described (4, 5).

Gene Array. Total RNA from mouse pancreatic islets, purified α-cell and β-cells, and acini was extracted using Absolutely RNA Microprep from Stratagene, while whole tissues and INS-1 β-cells were extracted using TRIzol (Gibco), followed by a cleanup with RNeasy columns (Qiagen). RNA was reverse transcribed into cDNA (SuperScript Choice System Invitrogen, using oligo(dT) primers and a T7 RNA polymerase promoter site); cDNA was *in vitro* transcribed and biotin-labeled (Affymetrix IVT labeling kit.) Quantity and quality of total RNA and cRNA profiles of all RNA preparations were analyzed, respectively using a NanoDrop ND-1000 spectrophotometer (NanoDrop Technologies) and 2100 Bioanalyzer (Agilent), the latter yielding distinct cRNA peaks corresponding to proinsulin and zymogen cRNA species for islets and acini, respectively (6) mRNA quantification was performed using Affymetrix mouse 430 2.0 expression microarrays: the overnight biotin-labeled cRNA was fragmented during 35 min at 94°C and hybridized during 16 h at 45°C, followed by washing/staining in a Fluidics Station (Affymetrix) and scanning using a 3000 GeneScanner. Raw data were analyzed using GCOS software. Signal intensities were scaled using the global scaling method taking 150 as target intensity value. For all tissues three independent biologic replicates were studied; islets and pituitaries were studied at $n = 5$.

RNA Extraction, PCR, and Quantitative RT-PCR. Total human and mouse islet RNA was extracted as described (2) and reverse transcribed. For quantitative PCR, RNA from rat α- and β-cells was extracted within 4 h from the start of the isolation, using RNAeasy (Qiagen) minicolums, according to the manufacturer's protocol. Commercially available human primers to glucagon, insulin, and 18S rRNA; rat primers to IL-6 receptor and gp130; and mouse primers to c-myc, p27, bcl-2, cyclin D1, D2, and D3 were purchased from Applied Biosystems and assayed according to the manufacturer's protocol using the ABI 7000 system (Applied Biosystems). Conventional PCR was performed using primers to the IL-6 receptor, gp130, tubulin, and GAPDH (Microsynth) (available upon request).

Glucagon and Insulin Secretion. α-cell function was assessed by 1h incubation with a basal (20 mM) and stimulated (2 mM) glucose concentration. Islet glucagon was extracted with 0.18 M HCl in 70% ethanol for determination of glucagon content. Glucagon was assayed by RIA (Linco). β-Cell function was assessed by 1h incubation with basal (2.8 mM) and stimulated (16.7 mM) glucose concentration. Islet insulin was extracted with 0.18 M HCl in 70% ethanol for determination of insulin content. Insulin was assayed by RIA (CIS Biointernational). In some experiments data were normalized to total islet protein content, measured using the BCA assay (Pierce). The IL-6 receptor antagonist, Sant 7, was used at 200 ng/ml.

Histochemical Analysis. For IL-6 receptor staining in mouse pancreatic sections and islets, rabbit anti-IL-6 receptor antibody (Santa Cruz), guinea-pig anti-glucagon antibody (Linco), and guinea-pig anti-insulin antibody (Dako) were used. Specificity was tested using isotype controls and blocking peptides. Further, this IL-6 receptor antibody was also used for Western blotting with respective recombinant proteins, HeLa cell extracts known to express the IL-6 receptor, and blocking peptides as controls. For Western blot analysis, mouse and human islet and purified rat α- and β-cell proteins were electrically transferred to nitrocellulose filters and incubated with IL-6 receptor (Santa Cruz), pSTAT3 and total STAT3 antibodies (Cell Signaling Technology). For proliferation studies, cells were stained with either a monoclonal Ki67 antibody (Zymed) or with a BrdU antibody (Roche). FACS sorted cells were co-stained with a BrdU antibody (Roche) and either a rabbit anti-glucagon (Dako) or a guinea pig anti-insulin antibody (Dako).

Proliferation of Purified α- and β-Cells. Sorted β-cells used for BrdU experiments were cultured on 804G-ECM, prepared as previously described (7), in DMEM (Gibco) containing 10% FCS, 11.2 mM glucose, and 110 μg/ml sodium pyruvate and supplemented with antibiotics. Aliquots of 3×10^5 cells were seeded in nonadherent, 100-mm diameter Petri dishes containing 9 ml medium. Cells were then incubated for 20 h at 37°C to allow full recovery of any cell surface molecules that may have been lost or damaged during islet isolation or cell purification. After recovery, cells were resuspended at a density of 4×10^5 cells/ml, and aliquots of 50 μl were plated as droplets on plastic dishes coated with 804G-ECM. After 24 h of culture on 804G-

ECM, BrdU (final concentration 10 μM) and IL-6 (100 ng/ml) were added to the cells for 48 h.

Islet Morphometry. Paraffin embedded pancreatic tissue sections were stained using guinea pig anti-insulin (Dako) and rabbit anti-glucagon (Dako) antibodies. Section area, and insulin and glucagon-positive cell area were determined from 3 pancreatic sections per animal, at 200-μm intervals, averaging 80–100 islets per animal using AxioVision (Zeiss) and Image J (NIH). Fraction of total endocrine cell area/total section area was multiplied by pancreatic weight to determine α- and β-cell mass.

Intraperitoneal Glucose and Insulin Tolerance Test. Mice were injected i.p. with 2 mg/g body weight glucose or 0.75 mU/g recombinant human insulin (Novo Nordisk). Blood samples were obtained from tail-tip bleedings, and blood glucose was measured with a glucometer (Freestyle). Homeostasis model for assessment of insulin resistance (HOMA-IR) was calculated as published (8).

Cytokines, Chemokines, and Hormones. Circulating cytokines, chemokines, insulin, and glucagon were assayed using a mouse Luminex kit (Linco).

Statistics. Data are expressed as means ± SEM. Significance was tested using Student's *t* test (2-tailed) and analysis of variance with Bonferonni's *post hoc* test ($P < 0.05$) for multiple comparison analysis.

1. Rouiller DG, Cirulli V, Halban PA (1990) Differences in aggregation properties and levels of the neural cell adhesion molecule (NCAM) between islet cell types. *Exp Cell Res* 191:305–312.
2. Maedler K, Fontana A, Ris F, Sergeev P, Toso C, *et al.* (2002) FLIP switches Fas-mediated glucose signaling in human pancreatic beta cells from apoptosis to cell replication. *Proc Natl Acad Sci USA* 99:8236–8241.
3. Sporeno E, Savino R, Ciapponi L, Paonessa G, Cabibbo A, *et al.* (1996) Human interleukin-6 receptor super-antagonists with high potency and wide spectrum on multiple myeloma cells. *Blood* 87:4510–4519.
4. Van De Winkel M, Pipeleers D (1983) Autofluorescence-activated cell sorting of pancreatic islet cells: Purification of insulin-containing B-cells according to glucose-induced changes in cellular redox state. *Biochem Biophys Res Commun* 114:835–842.
5. Bosco D, Meda P, Halban PA, Rouiller DG (2000) Importance of cell-matrix interactions in rat islet beta-cell secretion in vitro: Role of alpha6beta1 integrin. *Diabetes* 49:233–243.
6. Van Lommel L, *et al.* (2006) Probe-independent and direct quantification of insulin mRNA and growth hormone mRNA in enriched cell preparations. *Diabetes* 55:3214–3220.
7. Hammar EB, Irminger JC, Rickenbach K, Parnaud G, Ribaux P, Bosco D, Rouiller DG, Halban PA (2005) Activation of NF-kappaB by extracellular matrix is involved in spreading and glucose-stimulated insulin secretion of pancreatic beta cells. *J Biol Chem* 280:30630–30637.
8. Cai D, *et al.* (2005) Local and systemic insulin resistance resulting from hepatic activation of IKK-beta and NF-kappaB. *Nat Med* 11:183–190.

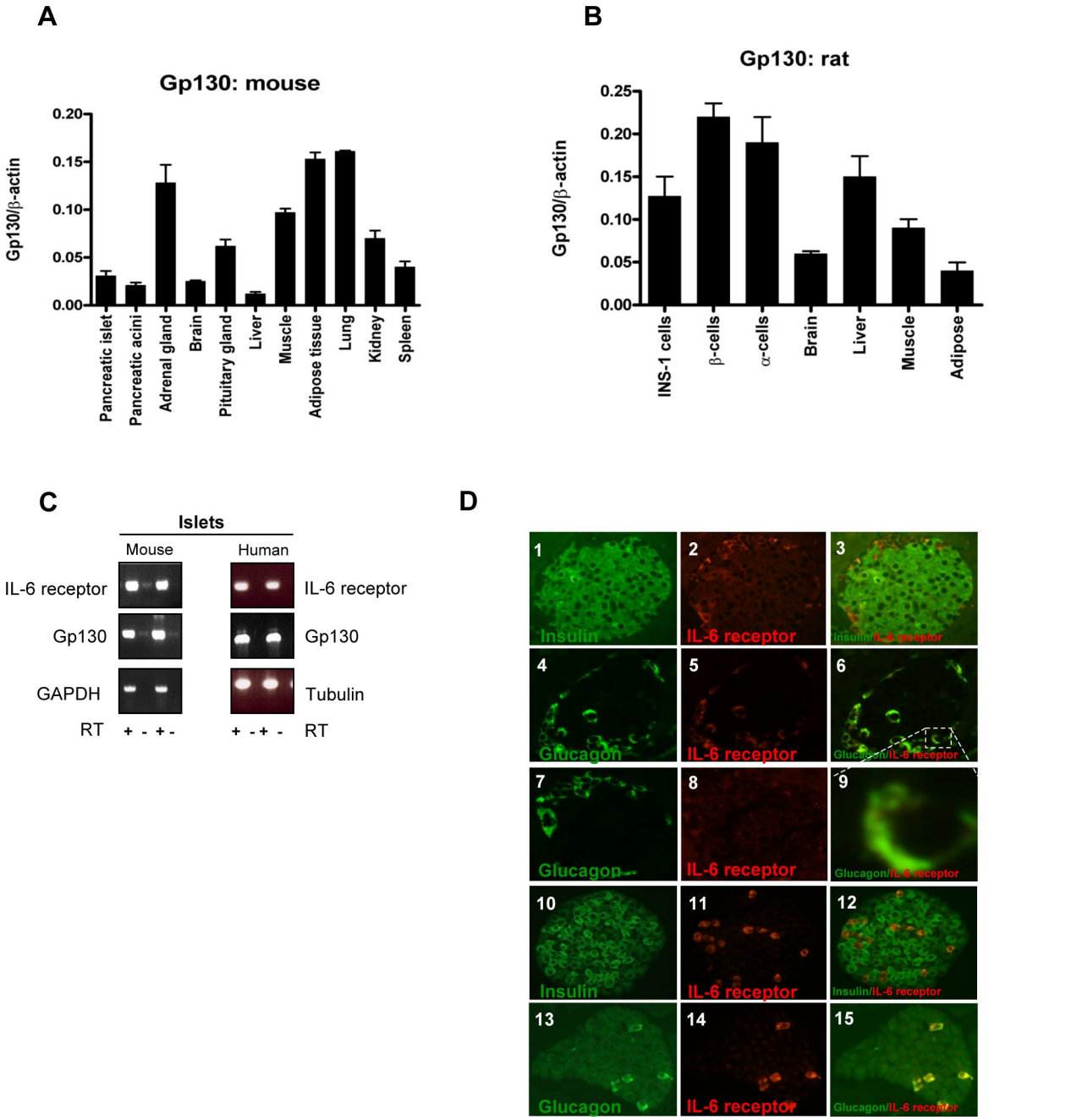

Fig. S1. IL-6R and gp130 expression in the pancreatic islet. Gp130 mRNA expression in mouse and rat tissues. (*A* and *B*) Tissue expression profile of mouse and rat gp130 mRNA expression determined by Affymetrix gene array ($n = 3–5$). (*C*) PCR on RNA extracted from mouse and human islets using primers to detect the IL-6R and gp130. (+) and (-) represent cDNA and RT negative control, respectively (representative of $n = 5$). (*D*) Immunostaining of the IL-6R (panels 2, 5, 8, 11, and 14) and the islet hormones insulin (panels 1, 10) and glucagon (panels 4, 7, and 13) on mouse pancreatic sections without (panels 1–6) and with preabsorption using IL-6R blocking peptide (panels 7, 8), and on cultured mouse islets (panels 10–15). Increased magnification of the overlay in panel 6 is shown in panel 9.

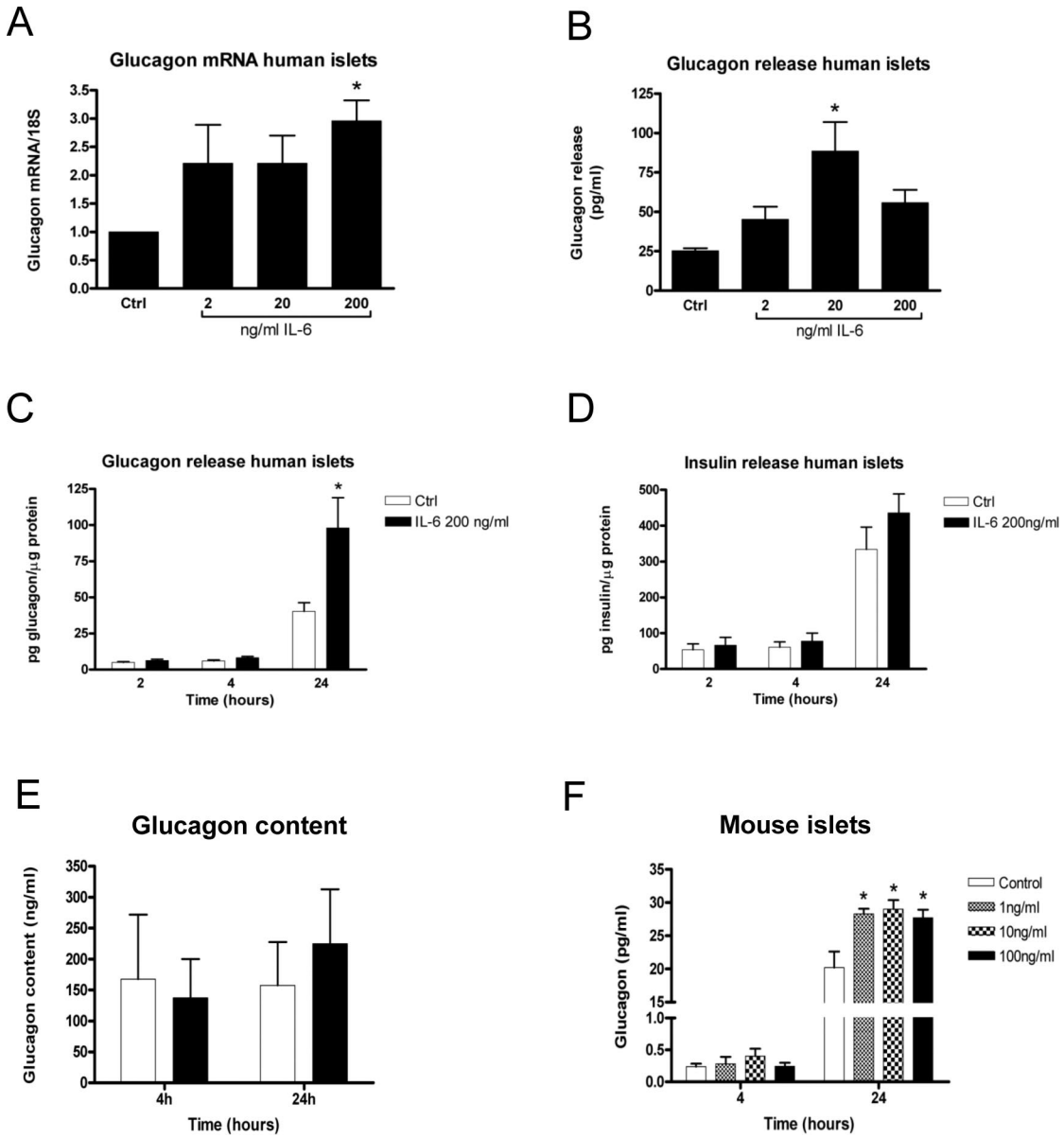

Fig. S2. IL-6 regulation of pro-glucagon mRNA, and glucagon and insulin release from human and mouse islets *in vitro*. (*A*) Pro-glucagon mRNA relative to 18S was measured in human islets after 4 h exposure to increasing doses of IL-6. (*B*) Glucagon release in culture medium of human islets (20 islets/well) after exposure to increasing doses of IL-6 for 24 h ($n = 3$). (*C*) Glucagon and (*D*) insulin release in culture medium of human islets after exposure to 200 ng/ml IL-6 for the indicated period. Release was normalized to total islet protein ($n = 3$). (*E*) IL-6 (200 ng/ml) regulation of glucagon content in human islets ($n = 4$). (*F*) IL-6 stimulates glucagon release in mouse islets *in vitro*. Glucagon release in culture medium of mouse islets after exposure to increasing doses of IL-6 for 24 h ($n = 3$). *, $P < 0.05$.

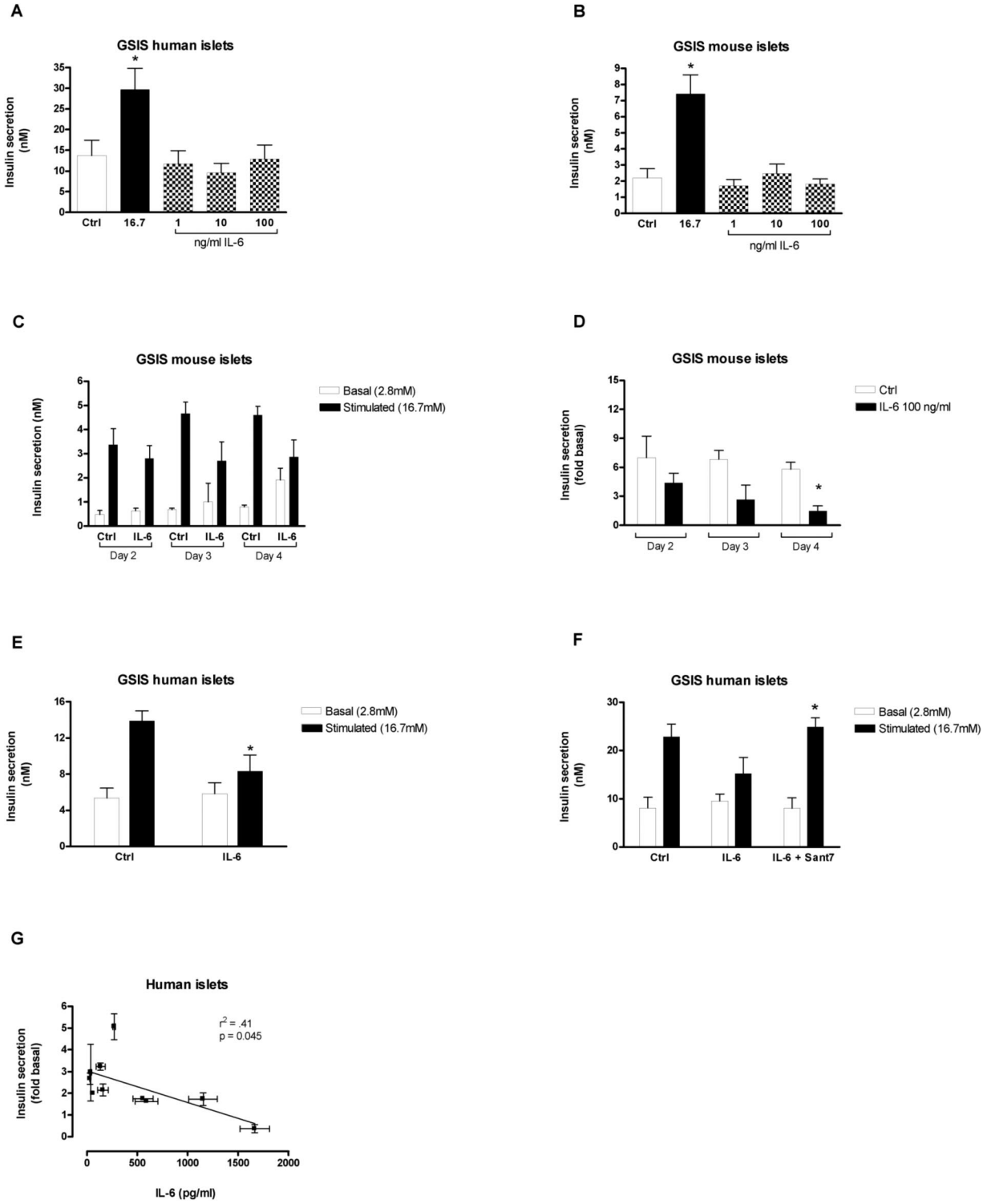

Fig. S3. IL-6 regulation of insulin secretion from mouse and human islets *in vitro*. (A) Human and (*B*) mouse islets were treated with increasing doses of IL-6 in the presence of 7.5 mM glucose (Ctrl) for 1 h and insulin secretion was assessed. 16.7 mM glucose (16.7) was used as a positive control to stimulate insulin secretion ($n = 3$). (C and D) Mouse islets were treated with 100 ng/ml IL-6 for 2, 3, and 4 days before assessment of glucose-stimulated insulin secretion. (*E* and *F*) Human islets were treated with IL-6 for 4 days in the absence (IL-6) and presence (Sant 7) of the IL-6 receptor antagonist, Sant 7, before assessment of glucose-stimulated insulin secretion (GSIS). (*G*) Glucose-stimulated insulin secretion (fold of high vs. low glucose) negatively correlated with increasing basal human islet IL-6 levels; the linear regression analysis is shown. *, $P < 0.05$.

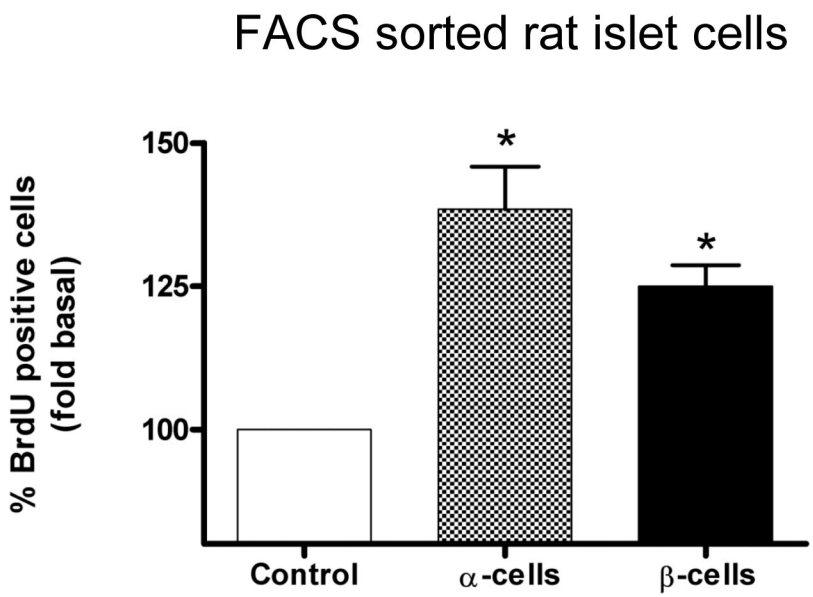

Fig. S4. IL-6 increases pancreatic α- and β-cell proliferation *in vitro*. % BrdU positive rat α- and β-cells of total number of cells. BrdU was added to cells for 2 days, in the absence and presence of 100 ng/ml IL-6 ($n = 3$). *, $P < 0.05$.

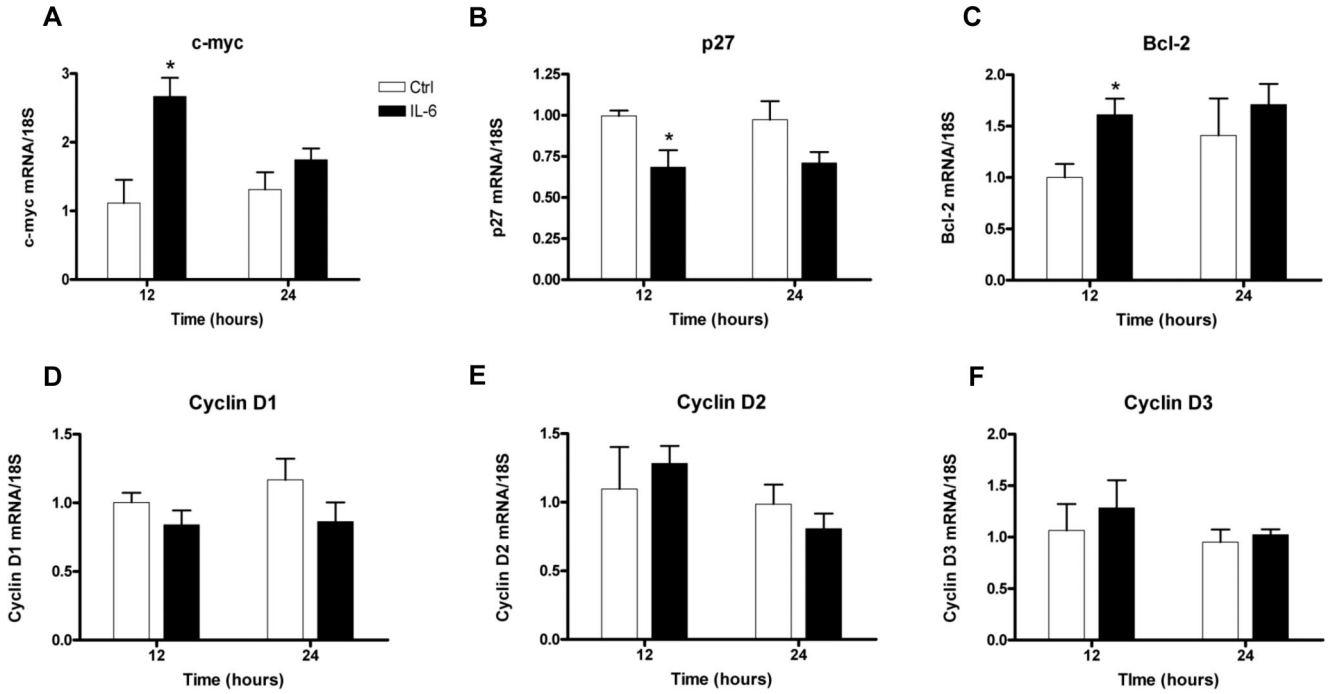

Fig. S5. Interleukin-6 induces proliferative and pro-survival genes in pancreatic islets. (*A*) c-myc, (*B*) p27, (*C*) bcl-2, (*D*) cyclin D1, (*E*) cyclin D2, and (*F*) cyclin D3 mRNA expression in mouse islets after exposure to IL-6 for 12 and 24 h. White bars, control; black bars, 100 ng/ml IL-6 ($n = 3$). ∗, $P < 0.05$.

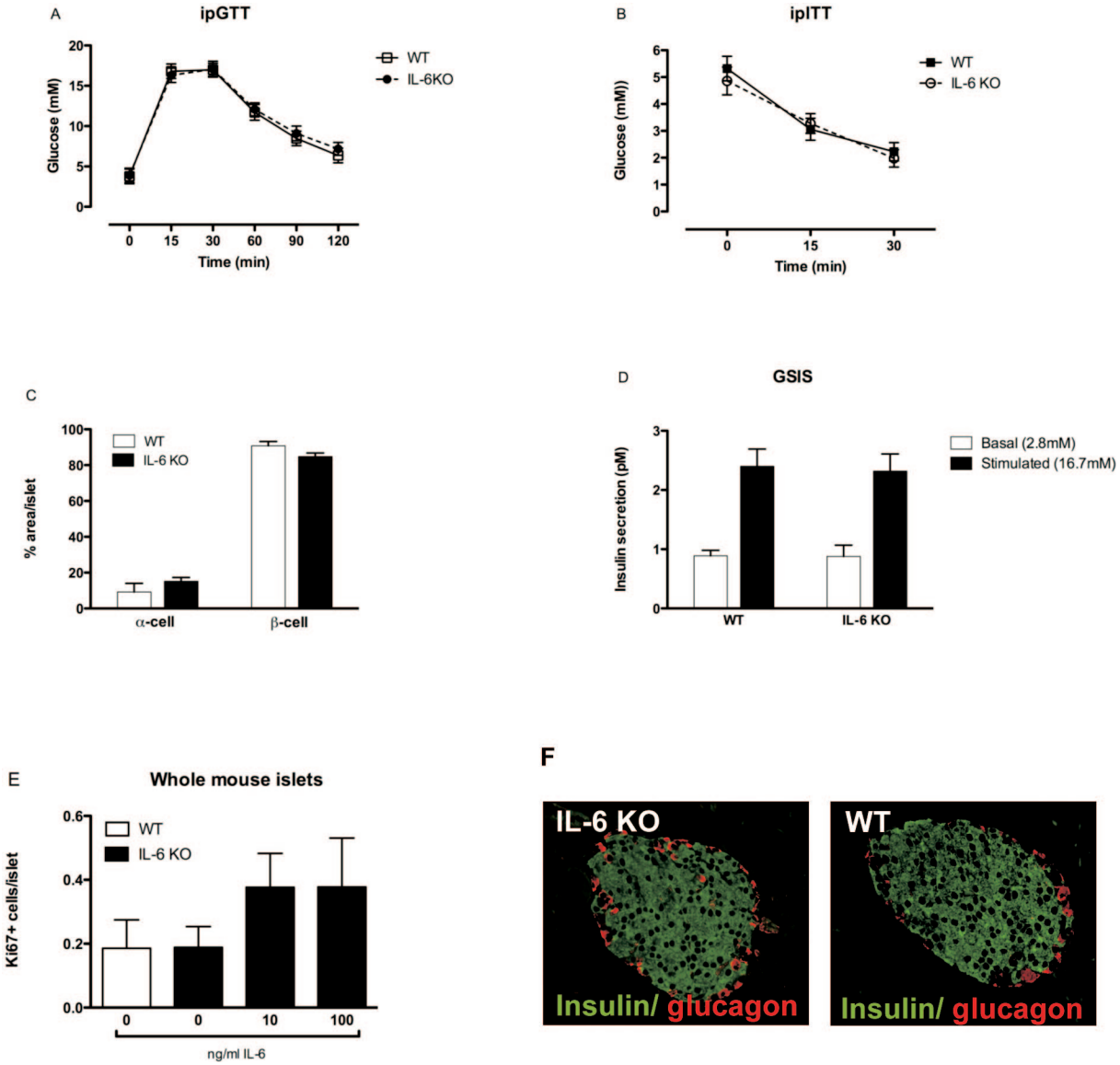

Fig. S6. Metabolic and islet phenotype in 10–12 week old WT and IL-6 KO mice on chow diet. (*A*) ipGTT in WT and IL-6 KO mice at 10–12 weeks of age (n = 20 for each group). (*B*) ipITT in WT and IL-6 KO mice at 10–12 weeks of age (n = 5 for each group). (*C*) % α-cell area/islet and % β-cell area/islet in WT and IL-6 KO mice (n = 5). (*D*) Glucose-stimulated insulin secretion from WT and IL-6 KO mice (n = 4). (*E*) Islet cell proliferation in response to IL-6 in WT and IL-6KO mice (n = 1). (*F*) Immunohistochemistry of a typical WT and IL-6KO islet stained for insulin and glucagon.

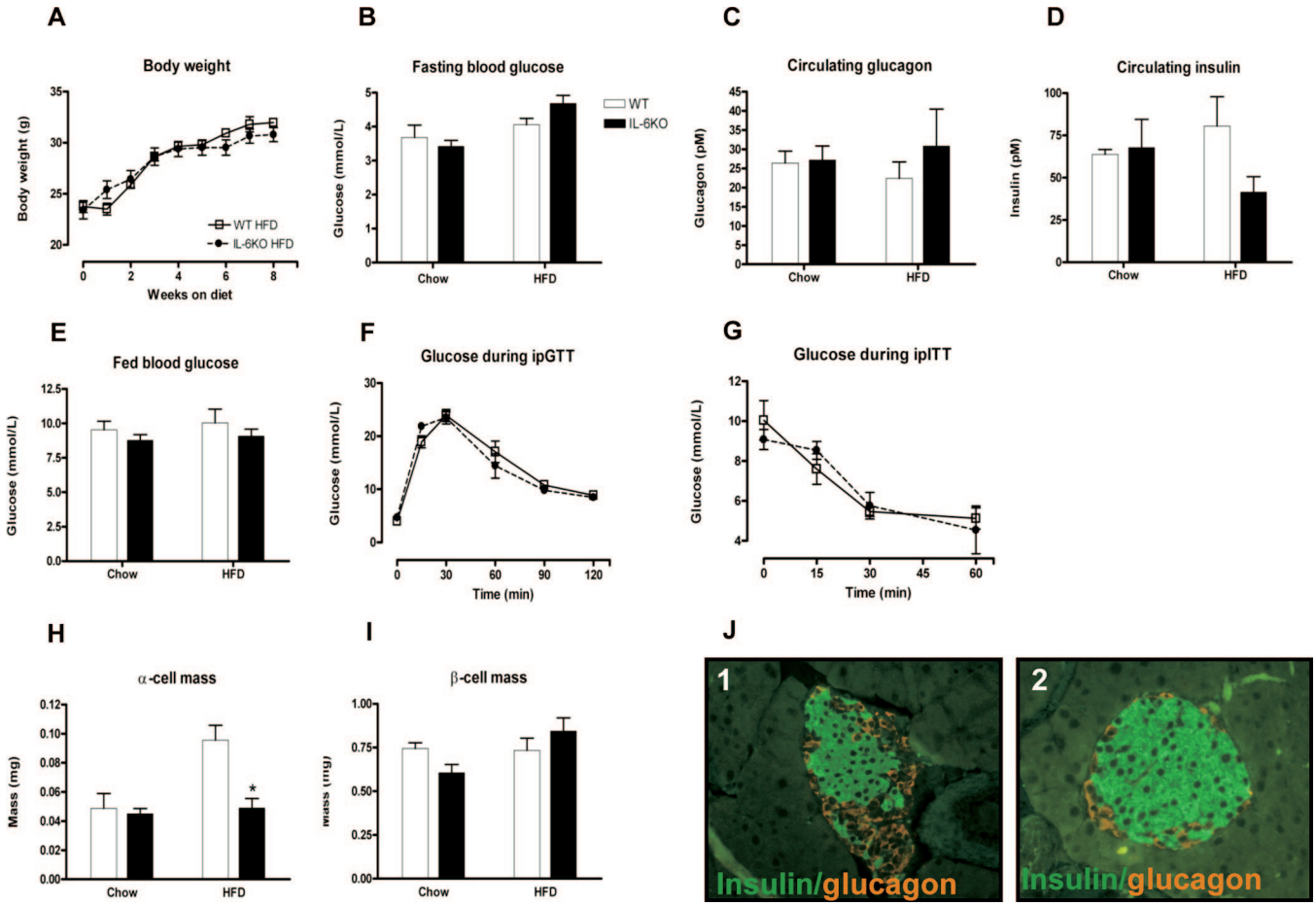

Fig. S7. Increased α-cell mass due to 8 week HF diet is IL-6-dependent. (*A*) Body weight, (*F*) ipGTT (glucose tolerance test) and (*G*) ipITT (insulin tolerance test) in WT (solid line, open squares) and IL-6 KO (dashed line, closed circles) mice fed HF diet for 8 weeks ($n = 4$ WT, $n = 5$ IL-6 KO). (*B*) Fasting blood glucose, (*C*) fasting plasma glucagon and (*D*) fasting plasma insulin, (*E*) random fed blood glucose, (*H*) α-cell mass, and (*I*) β-cell mass in WT and IL-6 KO after 8 weeks on HF diet (chow WT $n = 5$, chow IL-6 KO $n = 5$, HF WT $n = 4$, HF IL-6 KO $n = 5$). (*J*) Immunostaining of pancreatic sections from WT (panel 1) and IL-6 KO (panel 2) mice with insulin (green) and glucagon (red) after 8 weeks on HF diet. *, $P < 0.05$.

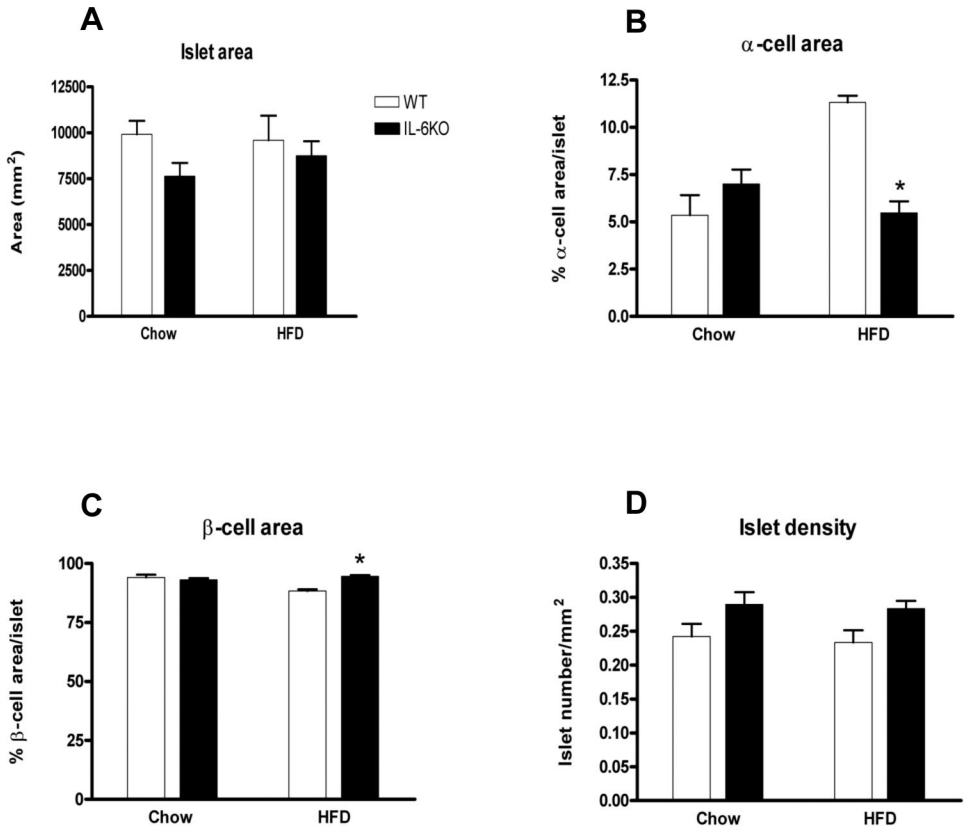

Fig. S8. Islet morphometry *in vivo* after 8 weeks of HF diet feeding. (*A*) Mean islet area, (*B*) percent α-cell area/islet, (*C*) percent β-cell area/islet, and (*D*) islet density in WT (white bars) and IL-6 KO (black bars) mice fed a chow or HF diet for 8 weeks. *, $P < 0.05$ compared with HF diet WT.

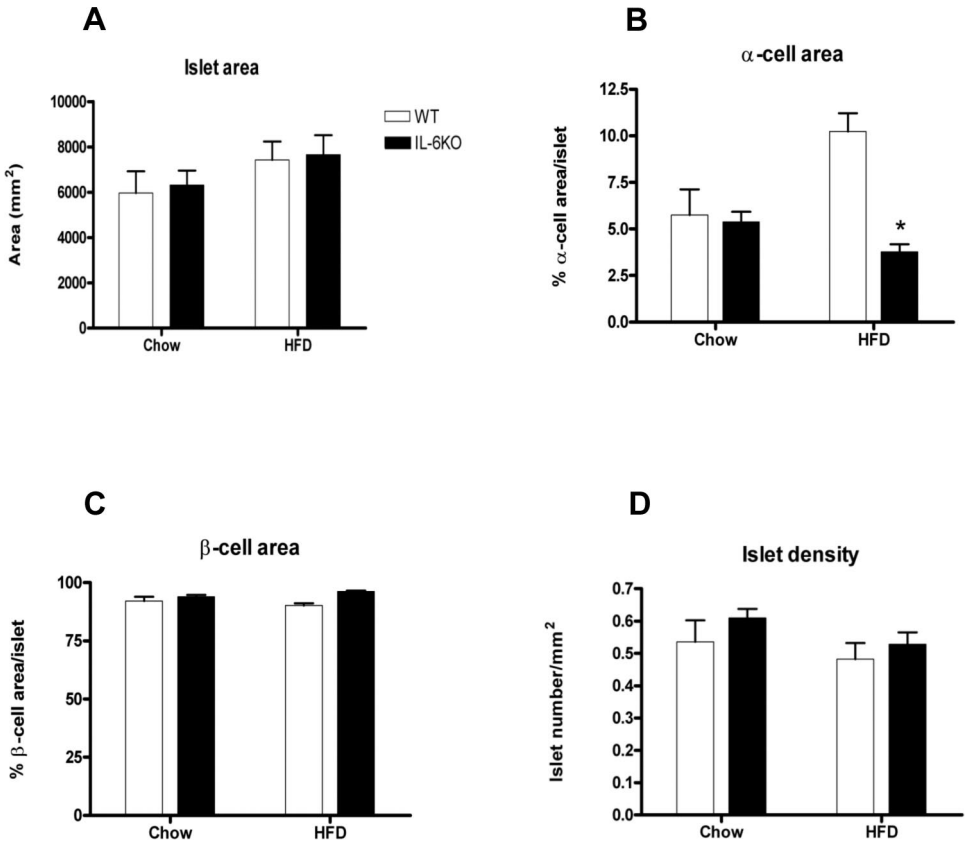

Fig. S9. Islet morphometry *in vivo* after 18 weeks of HF diet feeding. (*A*) Mean islet area, (*B*) percent α-cell area/islet, (*C*) percent β-cell area/islet, and (*D*) islet density in WT (white bars) and IL-6 KO (black bars) mice fed a chow or HF diet for 18 weeks. $*$, $P < 0.05$ compared with HF diet WT.